

# SYNCHROPHASOR APPLICATIONS OF THE NATIONAL ELECTRIC SYSTEM OPERATOR OF SPAIN

**S. López**

**Red Eléctrica de España**

**J. Gómez**

**Red Eléctrica de España**

**R. Cimadevilla**

**ZIV P+C**

**O. Bolado**

**ZIV USA**

## Summary

This paper examines a series of PMU (Phasor Measurement Unit) applications devised by the National Electric System Operator of Spain (Red Eléctrica de España - REE) including calculation of the sequence impedances of power lines, fault location in mixed lines, and monitoring of the system dynamic behavior. The paper covers in detail the problems of traditional algorithms and explains the advantages of the new algorithms based on synchrophasors. Examples include actual data from the grid.

## 1 INTRODUCTION

Power systems are becoming increasingly overloaded and fragile, reducing their stability margins. Environmental restrictions limit new construction to expand the transmission grid, and stipulate larger distance between generation and loads. On a separate front, market forces in the electric sector make utilities to maximize asset usage. These requirements, added to the rising quality of service demanded, entail improvements in the efficiency of power systems operation.

Phasor measuring units (PMUs) enable a number of different applications to improve the efficiency in power systems. This paper describes some of the applications devised by the National System Operator of Spain (Red Eléctrica de España, REE). Examples reviewed include:

- **Sequence Impedance Calculations for Transmission Lines:** traditional calculations based on line constants can result in significant errors, especially for zero sequence impedance. These errors will translate into incorrect settings on distance relays, fault locators, etc. Calculations based on measures by PMUs located on both ends of power lines provide a simple solution to obtain more accurate calculations.
- **Fault Location for Mixed Lines:** variations on zero sequence impedance in cables reduce the efficiency of traditional fault locators. Fault location based on measures by PMUs located in both ends of a mixed power line (combination of overhead and underground cable) gives more precise results.
- **Dynamic Behavior Monitoring of System:** Power system enlargement is creating small signal oscillations. Given the decreasing stability margins, knowledge of the dynamic behavior of the system is critical for proper operation. Using PMU readings from different points of a system, allows characterizing potential oscillations. This knowledge helps planners to devise corrective actions, increasing damping techniques and establishing defense procedures for unstable oscillations.

## 2 SEQUENCE IMPEDANCE CALCULATIONS FOR TRANSMISSION LINES

Traditionally, electric utilities calculate sequence impedances of power lines based on the geometric and electrical characteristics of the conductors. This method can give considerable errors, especially for the zero sequence impedance. These errors will translate into incorrect settings on distance relays, fault locators, etc.

Part of the data utilized for the calculations of positive sequence impedance are the permeability constants of the conductor and the environment, considered as equal ( $4\pi \times 10^{-7}$  H/m) since the conductor material is assumed to be fully paramagnetic. Even when using ferromagnetic conductors, as in the case of ACSR conductors (aluminum conductor steel reinforced), the approximation is utilized since the permeability variation is considered small. Also, the calculations involve the resistance of the conductor and a series of geometric parameters, such as radius and distance between conductors to obtain the GMR and the GMD, and the line length. If the line includes ground wires, the calculations require the resistance and the geometric arrangement of such wires [2]. These parameters include the following error sources:

- *Conductor Resistance*: This value varies with the temperature and the power flow. Some lines include sections with a different conductor type, therefore with different resistance per unit of length. Using a single resistance value in the impedance calculation program is therefore a source of errors.
- *Geometric parameters*: The conductor arrangement can differ from section to section due to different tower configurations; therefore the calculations usually are done with an average value. Also note that in many cases the exact cable lengths are unknown.

Regarding zero sequence impedance, in addition to the parameters above, calculations require the distance from the conductors to ground (geometric parameter also taken as an average), and the ground resistance (evaluated from empirical results by Carson, as a function of the frequency). Also is needed the ground resistivity [2], a piece of information hard to estimate accurately due to the non homogenous return path. Ground resistivity is affected by the soil composition, which changes along the line, by the humidity and the temperature. Below the freezing point, the water in the soil freezes with a dramatic reduction in humidity. Consequently, ground conditions are also dependent on the weather. On another aspect, ground composition studies do not take into account buried metallic objects, such as pipes, cables, etc.

Parallel circuits involve the calculation of the zero sequence mutual impedance. These calculations also involve all the parameters mentioned for individual zero sequence impedances, such as ground resistance and resistivity.

In general, sequence impedance calculations are dependent on a large number of parameters with significant sources of error.

Calculations of sequence impedances based on synchronized readings from two PMUs, one at each end of the line, allow for a simple method to obtain accurate results. Positive sequence impedance can be obtained anytime, derived from positive sequence currents and voltages at both ends of the line. Zero sequence impedance requires zero sequence currents and voltages; therefore it can only be obtained when there is a zero sequence flow. Such flow will be present during ground faults or serial faults (one or two open phases, impedance unbalances, etc.). In case of parallel circuits, zero sequence voltages and currents from both lines allow to derive the zero sequence mutual impedance.

Results obtained at a given time from PMU readings can be used to set all the devices with operating principles based on impedance metering. Nevertheless, since sequence impedances are subject to changes depending on the weather conditions and the power flow it is possible to get calculation under different conditions, with a programmed schedule for positive sequence impedance and during ground faults in the system for zero sequence impedance. If noticeable variations are detected between calculated and set values, it is possible to change the settings group of relays or fault locators, adapting those settings to the current conditions. To implement such adaptive schemes, the creation of different setting groups requires a previous study of historical records during a determined period of time.

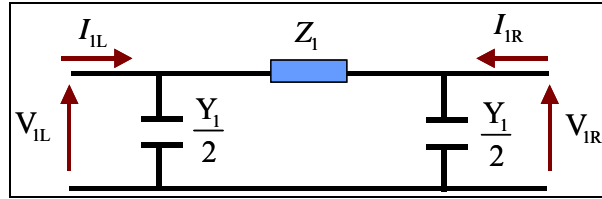
## 2.1 Positive Sequence Impedance Calculations

Figure 1 depicts the equivalent positive sequence PI circuit for a transmission line. The relationship among positive sequence currents and voltages at both ends of the line are included in the following equations:

$$V_{1R} = V_{1L} - (I_{1L} - V_{1L} \cdot \frac{Y_1}{2}) \cdot Z_1 \quad (1)$$

$$-I_{1R} = I_{1L} - V_{1L} \cdot \frac{Y_1}{2} - V_{1R} \cdot \frac{Y_1}{2} \quad (2)$$

From equation (2) it is possible to calculate  $Y_1 = 2 \cdot \frac{I_{1L} + I_{1R}}{V_{1L} + V_{1R}}$ . Substituting in (1)  $Z_1 = \frac{V_{1L}^2 - V_{1R}^2}{I_{1L} \cdot V_{1R} - I_{1R} \cdot V_{1L}}$



**Figure 1.** Positive sequence equivalent PI circuit for a transmission line

The previous calculations are valid for both overhead lines and cables. For long lines (approximately longer than 125 miles – 200 km – for overhead and 20 miles – 30 km – for cables) it is required to use a circuit of distributed parameters, in which the positive sequence voltage and current,  $v_1$  and  $i_1$ , respectively, in the point of the line located at a distance  $x$  from the local end, satisfy the following partial differential equations as a function of time:

$$-\frac{\partial u_1}{\partial x} = L_1 \cdot \frac{\partial i_1}{\partial t} + R_1 \cdot i_1$$

$$-\frac{\partial i_1}{\partial x} = C_1 \cdot \frac{\partial u_1}{\partial t} + G_1 \cdot u_1$$

where  $R_1$ ,  $L_1$ ,  $C_1$  and  $G_1$  represent positive sequence resistance, inductance, capacitance and conductance per length unit.

Solving the equations above on the frequency domain:

$$V_{1x} = V_{1L} \cdot ch(\gamma_1 \cdot x) - I_{1L} \cdot Z_{C_1} \cdot sh(\gamma_1 \cdot x)$$

$$-I_{1x} = I_{1L} \cdot ch(\gamma_1 \cdot x) - \frac{V_{1L}}{Z_{C_1}} \cdot sh(\gamma_1 \cdot x)$$

where  $\gamma_1 = \sqrt{(R_1 + j\omega L_1) \cdot (G_1 + j\omega C_1)} = \sqrt{z_1 \cdot y_1}$  and  $Z_{C_1} = \sqrt{\frac{(R_1 + j\omega L_1)}{(G_1 + j\omega C_1)}} = \sqrt{\frac{z_1}{y_1}}$  represent the propagation constant and the characteristic positive sequence impedance of the line, respectively.  $V_{1x}$  and  $I_{1x}$  represent the positive sequence voltage and current, as phasors, at a distance  $x$  from the local end (for  $x=L$ ,  $V_{1x}=V_{1R}$  and  $I_{1x}=I_{1R}$ ).

In this case, the real positive sequence impedance and admittance of the line ( $Z_1=z_1 \cdot L$  and  $Y_1=y_1 \cdot L$ ) can be calculated from the previous:

$$ZC_1 = \frac{V_{1L}^2 - V_{1R}^2}{\sqrt{(V_{1R}^2 - V_{1L}^2) \cdot (I_{1R}^2 - I_{1L}^2)}} \quad \text{and} \quad \gamma_1 = ch^{-1} \left( \frac{-V_{1L} \cdot I_{1L} + V_{1R} \cdot I_{1R}}{V_{1L} \cdot I_{1R} - V_{1R} \cdot I_{1L}} \right) \cdot \frac{1}{L}$$

Another possibility is to use the following equations once the parameters ( $Z_1'$  and  $Y_1'$ ) from the equivalent PI circuit are obtained [1]:

$$\frac{Y_1'}{2} = \frac{Y_1}{2} \cdot \frac{th\left(\frac{\gamma_1 \cdot L}{2}\right)}{\frac{\gamma_1 \cdot L}{2}} \quad (3) \quad Z_1' = Z_1 \cdot \frac{sh(\gamma_1 \cdot L)}{\gamma_1 \cdot L} \quad (4)$$

Note that the positive sequence impedance required by the company REE for most of their applications (distance relays, fault locators based on metering from a single line end, short-circuit calculations) is the impedance of the equivalent PI circuit ( $Z_1'$ ), since such applications, usually do not consider the line capacitance. Nevertheless, installation of PMUs in the grid is encouraging the use of fault locators based on distributed parameters, as the one described in section 3. These locators must use the real positive sequence impedance and admittance of the line.

## 2.2 Zero Sequence Impedance Calculations

Zero sequence impedances will be calculated when ground faults occur. Such faults can be internal or external to the line. For internal faults, the first piece of information required is the distance to the fault, which could be calculated with a positive sequence circuit similar to the one in section 3, but simplified since the line is not mixed. With the distance value and using the zero sequence circuit, it is possible to calculate the zero sequence impedance, but this calculated impedance is not considered for internal faults. It has been demonstrated that the zero sequence impedance is largely affected by the accuracy of the distance to the fault calculations, with small errors in the first calculation giving large errors in the second one. If the fault is external to the line it is not needed to calculate the distance to the fault. On the other hand, it has to be taken into account that, in general, there will be more instances of external faults than internal ones. Figure 2 depicts the equivalent zero sequence PI circuit of a line for an external fault.

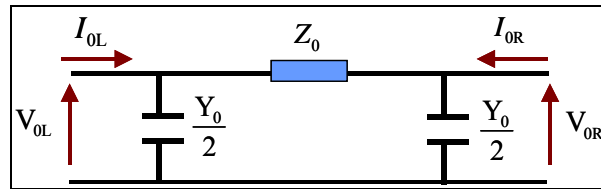


**Figure 2.** Zero sequence equivalent PI circuit for a transmission line

Using formulas similar to the ones included in the previous section, it is possible to calculate the zero sequence impedance and admittance:

$$Z_0 = \frac{V_{0L}^2 - V_{0R}^2}{I_{0L} \cdot V_{0R} - I_{0R} \cdot V_{0L}} \quad Y_0 = 2 \cdot \frac{I_{0L} + I_{0R}}{V_{0L} + V_{0R}}$$

The previous calculations are valid for both overhead lines and cables, although results for cables will vary depending on the return path of the current (by the shield, ground or both). In case of long lines, it is possible to obtain, similar to the previous section, the real zero sequence impedance and admittance of the line.

For parallel lines, it is possible to calculate the zero sequence mutual impedance. Figure 3, depicts the zero sequence circuit of parallel lines. Considering the equivalent PI circuit for each line, the zero sequence mutual admittance is assumed to be concentrated in both ends of the line. In such circuit the following equations are satisfied:

$$V_{0R} = V_{0L} - \left[ I_{0L} - V_{0L} \cdot \frac{Y_0}{2} - (V_{0L} - V_{0L}') \cdot \frac{Y_{0M}}{2} \right] \cdot Z_0 - \left[ I_{0L}' - V_{0L}' \cdot \frac{Y_0'}{2} - (V_{0L}' - V_{0L}) \cdot \frac{Y_{0M}}{2} \right] \cdot Z_{0M} \quad (5)$$

$$-I_{0R} = I_{0L} - V_{0L} \cdot \frac{Y_0}{2} - (V_{0L} - V_{0L}') \cdot \frac{Y_{0M}}{2} - V_{0R} \cdot \frac{Y_0}{2} - (V_{0R} - V_{0R}') \cdot \frac{Y_{0M}}{2} \quad (6)$$

$$V_{0R}' = V_{0L}' - \left[ I_{0L}' - V_{0L}' \cdot \frac{Y_0'}{2} - (V_{0L}' - V_{0L}) \cdot \frac{Y_{0M}}{2} \right] \cdot Z_0' - \left[ I_{0L} - V_{0L} \cdot \frac{Y_0}{2} - (V_{0L} - V_{0L}') \cdot \frac{Y_{0M}}{2} \right] \cdot Z_{0M} \quad (7)$$

$$-I_{0R}' = I_{0L}' - V_{0L}' \cdot \frac{Y_0'}{2} - (V_{0L}' - V_{0L}) \cdot \frac{Y_{0M}}{2} - V_{0R}' \cdot \frac{Y_0'}{2} - (V_{0R}' - V_{0R}) \cdot \frac{Y_{0M}}{2} \quad (8)$$

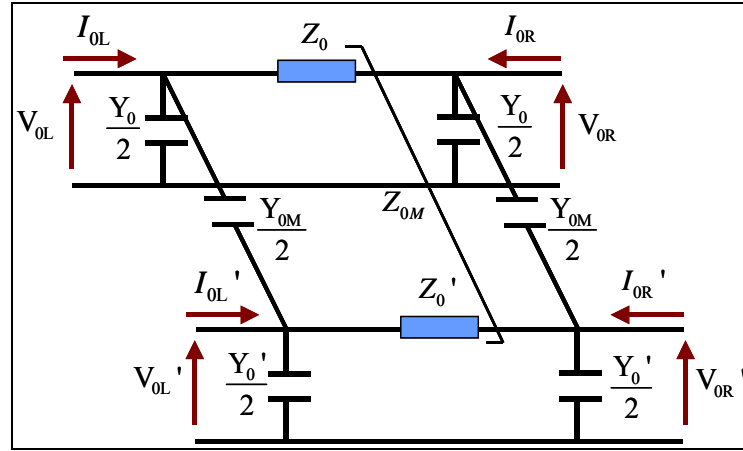


**Figure 3.** Zero sequence equivalent PI circuit for parallel lines

Having 4 equations with 6 unknowns ( $Y_0$ ,  $Y_0'$ ,  $Y_{0M}$ ,  $Z_0$ ,  $Z_0'$  and  $Z_{0M}$ ) it is required to record zero sequence measurements in two different moments (two different ground faults) to obtain double the number of equations.

In case of long parallel circuits, the zero sequence coupling between lines prevents solving the differential equations directly. The best method to obtain the mutual impedance is via the Clarke transformation for parallel lines which allows decoupling the circuits in every mode [13]. Nevertheless, in the actual applications of REE, the calculations based on a circuit of concentrated parameters are considered to be valid.

For non-transposed lines, if we require higher accuracy in calculating the sequence impedances, it is possible to solve the nine unknowns, elements of the sequence impedance matrix, with the three equations given by the three sequence networks, by getting measurements in three different instances. In this case it is not required to wait for a fault to calculate the zero sequence since unbalances in the line produce a zero sequence flow.

If the lines are non-transposed and long, the calculations get more complex since it is required solving the differential equations that use the phase impedance and admittance matrices, coupled between them. Decoupling such equations is done using the modal theory, transforming the phase magnitudes to modal magnitudes [13]. This requires defining the transformation matrix (Eigen vector matrix). The values in this matrix are not constant but depend on the phase impedance and admittance matrices. The problem is that, in this case, the values of these matrices are unknown.

### 2.3 Simulation

To test the algorithms described, simulations are run in a RTDS system (Real Time Digital Simulator). The simulations include two 220kV lines of 30 and 190 miles (50 and 300 km), and a 220 kV parallel line with 60 miles (100 km). The test simulates different conditions: different source impedances, load flows, and for zero sequence calculations, different ground faults with different fault ground resistance.

Metering at both line ends where recorded with ZIV distance relays including PMU functionality. The relays calculate 50 synchrophasors per second with a nominal frequency of 50 Hz, using one cycle recursive Fourier transform with 32 samples per cycle. To maintain accuracy at off-nominal frequencies, the sampling rate is determined according to the measured frequency in the grid [12]. Since the sampling rate is not synchronized with the signal delivered by the GPS clock (PPS – Pulse per second), to obtain the synchrophasor angle, an algorithm is used to compensate for the existing phase difference between the cosine wave used by the Fourier transform (wave defined by the cosine coefficients, with the maximum coincident with coefficient number zero) and the cosine wave defined by the GPS (with the maximum coincident with the PPS). With this technique the TVE (Total Vector Error) achieved is less than 1% in the range of 40 to 70 Hz.

To eliminate the DC offset component of the fault current, the PMUs apply a digital filter before processing the samples in the Fourier transform. Such filter limits to 3% the transient overreach, introducing a delay less than a  $\frac{1}{4}$  cycle.

The PMUs include antialiasing digital filters to eliminate interference signals capable of aliasing the calculation frequency for 50 synchrophasors per second. Since such filters consider a calculation window longer than a cycle, they are disabled for this particular application, to record suitable fault values.

Fault values, required for the zero sequence impedance metering, are recorded according to a highly sensitive fault detection unit, which operates on variations of the sequence currents. If the time between the activation of this unit and the first fraction of a second received is less than half a cycle, the synchrophasor stored is the one corresponding to the next fraction of a second received. If such time is longer than half a cycle the synchrophasor stored is the one corresponding to the first fraction of a second received. Using this criteria and with the synchrophasors calculated half cycle after the fraction of a second (in order to center the calculation window) the fault values considered are those 1 or 2 cycles after the activation of the fault detector.

TYPE OF CIRCUIT	LENGTH	PARAMETERS
SIMPLE	L1=50 km	$z1 = 0.0717 + j \cdot 0.4135 \ \Omega/\text{Km}$ $z0 = 0.3029 + j \cdot 1.2471 \ \Omega/\text{Km}$
	L2=300 Km	$y1 = j \cdot 2.8 \ \mu\text{S}/\text{Km}$ $y0 = j \cdot 1.97 \ \mu\text{S}/\text{Km}$
DOUBLE	L3=100 km	$z0M = 0.25 + j \cdot 0.76 \ \Omega/\text{Km}$ $y0M = j \cdot 1.4 \ \mu\text{S}/\text{Km}$

*Table 1. Parameters for the simulated lines*

### 2.3.1 Results without external errors

Tables 2, 3 and 4 include the positive and zero sequence impedance calculation results, without considering errors external to the PMUs, and without DC component in the faults. It is possible to observe that the errors in the reactance calculations are less than 3%. Note that this parameter is the one with larger error sources using the traditional method.

LÍNE	ZSOURCE (ohms)	LOAD CURRENT	RESISTANCE ERROR	REACTANCE ERROR	ADMITANCE ERROR
1	1	0.5 A	8.9%	0.62%	-13.21%
1	20	1.5 A	5.43%	-0.09%	-12.05%
2	1	0.5 A	3.8%	1.10%	3.37%
2	20	1.5 A	1.1%	0.77%	5.85%

*Table 2. Positive sequence parameter metering results*

LÍNE	FAULT TYPE	ZSOURCE (ohms)	LOAD CURRENT	FAULT RESISTANCE (ohms)	RESISTANCE ERROR	REACTANCE ERROR	ADMITANCE ERROR
1	AG	1	0.5 A	50	1.25%	-0.53%	10.1%
1	BCG	20	1.5 A	10	2.5%	0.024%	-9.4%
2	AG	1	0.5 A	50	2.8%	2.3%	9.9%
2	BCG	20	1.5 A	10	0.17%	1.8%	-12.8%

*Table 3. Zero sequence parameter metering results for single circuit*

LÍNE	FAULT TYPE	ZSOURCE (ohms)	LOAD CURRENT	FAULT RESISTANCE (ohms)	MUTUAL RESISTANCE ERROR	MUTUAL REACTANCE ERROR	MUTUAL ADMITTANCE ERROR
3	AG	1	0.5 A	50	5.3%	2.8%	13.4%

*Table 4. Zero sequence parameter metering results for parallel circuits*

### 2.3.2 Results with external errors

The following sections include the sequence impedance calculation results for lines 1 and 2, considering one of the previous simulated conditions (1.5A load, 20 ohm source impedance, and BCG fault for the zero sequence calculation), and, taking into account, this time, synchronization and instrument transformers errors. Also, the influence of the DC component in the faults is analyzed.

#### 2.3.2.1 Influence of synchronization between ends

Table 5 lists the additional errors in the metering of positive and zero sequence resistance, reactance and admittance when a 10° phase difference is added to the currents measured by both PMUs. Table 6 lists those errors when the 10° phase difference is added to the voltages.

The significant errors recorded in the positive sequence reactance show the need for a precise synchronization between the ends. This accuracy is guaranteed by the usage of accurate GPS clocks. It is important to check that the synchrophasors used for the impedance calculations include a suitable indication of the time quality.

It is important to remark that the higher the voltage magnitudes are, the higher the influence of the synchronization error is. So the errors in the positive sequence reactance will be reduced if this parameter is

calculated during fault conditions (together with the zero sequence impedance) instead of during load conditions. However, as the faults injected in the tests performed were very resistive ones, the fault voltage magnitudes were very close to the nominal, so the errors obtained for calculations during fault conditions were still high. For this type of faults it is more convenient to calculate the positive sequence reactance based on pure fault values.

Table 6b includes the errors in the resistance, reactance and admittance for positive sequence impedance calculations based on pure fault values, using the recorded values for the zero sequence calculations. As it can be seen, the errors are very small.

POSITIVE SEQUENCE				ZERO SEQUENCE			
LINE	ADDITIONAL RESISTANCE ERROR	ADDITIONAL REACTANCE ERROR	ADDITIONAL ADMITTANCE ERROR	LINE	ADDITIONAL RESISTANCE ERROR	ADDITIONAL REACTANCE ERROR	ADDITIONAL ADMITTANCE ERROR
1	67.14%	-1.97%	606.95%	1	70.27%	-4.87%	-1396.10%
2	60.34%	-2.94%	62.48%	2	80.05%	-5.07%	-49.31%

*Table 5. Influence of a 10° synchronizing error between currents*

POSITIVE SEQUENCE				ZERO SEQUENCE			
LINE	ADDITIONAL RESISTANCE ERROR	ADDITIONAL REACTANCE ERROR	ADDITIONAL ADMITTANCE ERROR	LINE	ADDITIONAL RESISTANCE ERROR	ADDITIONAL REACTANCE ERROR	ADDITIONAL ADMITTANCE ERROR
1	44.00%	190.00%	-1.49%	1	6.06%	-0.26%	-4.83%
2	-30.04%	45.55%	3.76%	2	1.02%	-0.03%	-0.07%

*Table 6. Influence of a 10° synchronizing error between voltages*

POSITIVE SEQUENCE			
10° ERROR BETWEEN VOLTAGES			
LINE	ADDITIONAL RESISTANCE ERROR	ADDITIONAL REACTANCE ERROR	ADDITIONAL ADMITTANCE ERROR
1	5.20%	-0.14%	-0.044%
2	0.85%	-0.02%	0.00%

*Table 6b. Influence of a 10° synchronizing error between voltages based on pure fault metering values*

### 2.3.2.2 Influence of instrument transformers

REE uses the following instrument transformers:

- Current Transformers **5P20**: per standard IEC 44-1, with limit errors for magnitude and angle of 1% and 60 minutes, respectively, at rated current; for currents 20 times rated the composite error must be below 5%.
- Voltage transformers **3P**: per standard IEC 60044-2, with limit errors for magnitude and angle 3% and 120 minutes, respectively, at 5% rated voltage and at the rated voltage multiplied by the rated voltage factor (1.2, 1.5 or 1.9).

To consider the errors introduced by the instrument transformers, 3% and 2° errors are added to the magnitudes and angles, respectively, of the currents and voltages measured by the PMUs. The worst case scenario has been considered for both the impedance and admittance calculations:

- a) +3% for  $I_{\text{local}}$  / +3% for  $I_{\text{remote}}$  and +2° for  $I_{\text{local}}$  / +2° for  $I_{\text{remote}}$  for impedance calculation
- b) +3% for  $I_{\text{local}}$  / -3% for  $I_{\text{remote}}$  and +2° for  $I_{\text{local}}$  / -2° for  $I_{\text{remote}}$  for admittance calculation
- c) +3% for  $V_{\text{local}}$  / +3% for  $V_{\text{remote}}$  and +2° for  $V_{\text{local}}$  / +2° for  $V_{\text{remote}}$  for admittance calculation
- d) +3% for  $V_{\text{local}}$  / -3% for  $V_{\text{remote}}$  and +2° for  $V_{\text{local}}$  / -2° for  $V_{\text{remote}}$  for admittance calculation

Such errors have been directly introduced in the positive and zero sequence measurement, considering an equal error in the phase magnitudes. However, errors with opposite sign in the phase magnitudes can generate much larger errors in the zero sequence magnitudes, mainly in the voltage. The usage of zero sequence pure fault magnitudes reduce significantly the voltage errors, given that these errors remain stable (percentage-wise for magnitude errors, and absolute-wise for angle errors) between pre-fault and fault conditions. This stability requires that the voltage transformer error curves display little dispersion in the whole metering range.

Tables 7, 8, 9 and 10 include the additional measuring errors for resistance, reactance and admittance when the previous described error combinations are introduced. The results uncover the need for calibrating the PMUs based on the transformer error curves, to calculate accurate line impedances, mainly for positive sequence.

It is worth to note that positive sequence parameter calculations based on fault or pure fault values (depending on the fault voltage magnitude) reduce significantly the previous errors.

POSITIVE SEQUENCE				ZERO SEQUENCE			
LINE	ADDITIONAL RESISTANCE ERROR	ADDITIONAL REACTANCE ERROR	ADDITIONAL ADMITTANCE ERROR	LINE	ADDITIONAL RESISTANCE ERROR	ADDITIONAL REACTANCE ERROR	ADDITIONAL ADMITTANCE ERROR
1	4.85%	-2.99%	35.76%	1	-2.94%	-2.91%	59.33%
2	0.77%	-3.98%	6.39%	2	-2.91%	-2.91%	53.90%

**Table 7.** Influence of a 3% error in the current magnitudes

POSITIVE SEQUENCE				ZERO SEQUENCE			
LINE	ADDITIONAL RESISTANCE ERROR	ADDITIONAL REACTANCE ERROR	ADDITIONAL ADMITTANCE ERROR	LINE	ADDITIONAL RESISTANCE ERROR	ADDITIONAL REACTANCE ERROR	ADDITIONAL ADMITTANCE ERROR
1	38.85%	-1.18%	-52.95%	1	22.88%	-1.33%	-634.74%
2	36.72%	-2.09%	39.16%	2	24.72%	-1.24%	-23.14%

**Table 8.** Influence of a 2° error in the current angle

POSITIVE SEQUENCE				ZERO SEQUENCE			
LINE	ADDITIONAL RESISTANCE ERROR	ADDITIONAL REACTANCE ERROR	ADDITIONAL ADMITTANCE ERROR	LINE	ADDITIONAL RESISTANCE ERROR	ADDITIONAL REACTANCE ERROR	ADDITIONAL ADMITTANCE ERROR
1	390.14%	-10.90%	-2.90%	1	-3.57%	-3.47%	-2.92%
2	105.34%	-3.66%	-0.35%	2	-3.07%	-3.07%	-2.92%

**Table 9.** Influence of a 3% error in the voltage magnitudes

POSITIVE SEQUENCE				ZERO SEQUENCE			
LINE	ADDITIONAL RESISTANCE ERROR	ADDITIONAL REACTANCE ERROR	ADDITIONAL ADMITANCE ERROR	LINE	ADDITIONAL RESISTANCE ERROR	ADDITIONAL REACTANCE ERROR	ADDITIONAL ADMITANCE ERROR
1	119.42%	29.47%	-1.26%	1	26.26%	-1.55%	-21.63%
2	32.43%	26.23%	2.18%	2	25.32%	-1.26%	-2.08%

**Table 10.** Influence of a 2° error in the voltage angle

### 2.3.2.3 Influence of the incidence angle

In the worst case scenario (current readings 1 cycle after the activation of the fault detector and maximum DC component), the current error is 1% in the magnitude and 3° in the angle. If the currents in both ends have the same error, the additional errors in the zero sequence resistance and reactance will be 21.66% and 2.30%, respectively for line 1, and 21.48% y -2.26%, respectively for line 2. If the current error is only in one end, the zero sequence admittance error would be 10.24% for line 1 and 2.46% for line 2. To reduce these errors it is required to increase the time from the fault detector activation until the fault readings are recorded. This time increase will be possible if the fault clearing time is long enough. Therefore, the protective relay and the adjacent line circuit breaker operating times must be considered.

## 3 FAULT LOCATION IN MIXED LINES

The significant growth of urban areas in Spain has caused a noticeable increase of partial power line burying, expanding the number of mixed lines in the REE portfolio. These mixed lines have a considerable shorter underground section as compared with the overhead section (cable is less than 15-20% of the overhead section) therefore, reclosing is used to recover from transient overhead faults. Cable faults, on the other hand, should not be reclosed, first, as a measure of public safety, since many faults are caused by crews operating machinery in the vicinity of the cable. On the other hand, note that cable faults are mainly permanent faults, with reclosing worsening the existing damages.

To detect the faulted section, the overhead or the underground, the original solution used in every mixed line was to install two line differential relays at both ends of the cable. The differential relay operation sends, via communications, a block signal to the reclosers located at both ends of the mixed line. Such solution has the inconvenience of requiring current transformers, DC power, etc., at both ends of the cable with the consequent increase in cost of both the installation and the maintenance. Another solution currently used, is the installation of distance relays at both ends of the mixed line with a specific zone to detect faults in the overhead section. Reclosing is subject to the operation of any of these two distance zones. This second solution is much more economical than the previous one, since it does not require protective relays at the ends of the cable. The disadvantage of the second approach is that the distance zones, used to detect overhead faults, cannot cover 100% of the overhead section due to the possible overreaching effect by the following factors: the mixed nature of the fault loop when the fault is located in the cable or in the next overhead section (the zero sequence compensation for overhead lines is very different of the one for cables); the lack of consideration of the line capacitance; the inaccuracies of the zero sequence impedance value of the overhead section; the non-homogenous nature of the system and the load flow in the line for resistive faults; possible errors in the selection of fault type; etc. The usual distance zone reach is set to 85-90% of the positive sequence impedance of the overhead section. Therefore, many of the faults in the overhead section not covered will be undetected by the distance zones and tripped without reclosing. Even faults located in the covered zone can be undetected in case of underreach effects, present on very resistive faults.

The operation of the distance zones covering the overhead section can be complemented with a fault locator, which has a longer operating time to perform calculations, but is able to pinpoint the faulted section. This

information can be sent to the control center, and in cases where the fault is located in the overhead section outside the distance protection zones, a manual close can be done in a relatively short time. Nevertheless, REE practices intent to locate the faulted section based solely on the fault locator, which should perform its calculations before the reclosing sequence is completed, being able to abort the cycle in case of faults in the cable. In this final solution, all instantaneous trips would initiate the reclosing sequence.

Fault locators based on measurements at one end of the line do not provide good results, since the algorithms require the use of the zero sequence impedance of the cable, which varies depending on the current return path on ground faults. Fault location based on metering by two PMUs located at both ends of the line can rely only on the positive sequence network, eliminating the problem described. Since the positive sequence network is used in every fault, there is no need to determine the fault type. As an added bonus, the algorithm is not affected by the fault resistance, load flow and the non-homogenous nature of the system.

Given the variation of the positive sequence impedance of the line, mainly on the overhead section, the fault locating algorithms must use different circuits depending on the faulted section. Figures 4 and 5 show the circuits to consider for faults in the first overhead section and the cable, respectively.

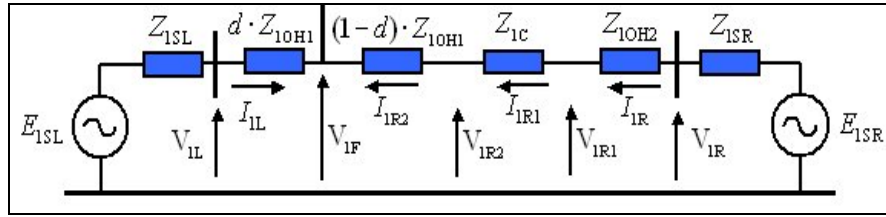


**Figure 4.** Positive sequence network for faults in the first overhead section

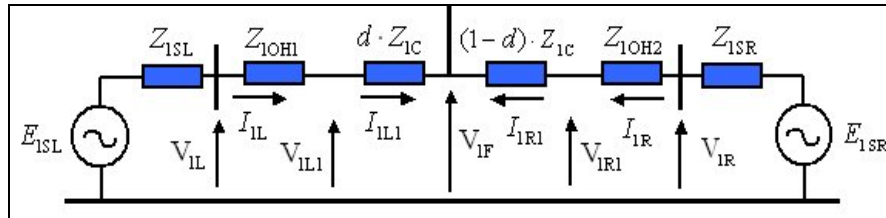


**Figure 5.** Positive sequence network for faults in the cable

The equations pertaining to these circuits are included below. To take into account the capacitance of the cable and the overhead sections, distributed parameter circuits are considered.

#### Fault in the first overhead section

$$V_{1F} = V_{1L} \cdot ch(\gamma_{L1} \cdot d \cdot L_{L1}) - I_{1L} \cdot Z_{C_{L1}} \cdot sh(\gamma_{L1} \cdot d \cdot L_{L1})$$

$$V_{1F} = V_{1R2} \cdot ch[\gamma_{L1} \cdot (1-d) \cdot L_{L1}] - I_{1R2} \cdot Z_{C_{L1}} \cdot sh[\gamma_{L1} \cdot (1-d) \cdot L_{L1}]$$

$$V_{1R2} = V_{1R1} \cdot ch(\gamma_C \cdot L_C) - I_{1R1} \cdot Z_{C_C} \cdot sh(\gamma_C \cdot L_C) \quad I_{1R2} = I_{1R1} \cdot ch(\gamma_C \cdot L_C) - \frac{V_{1R1}}{Z_{C_C}} \cdot sh(\gamma_C \cdot L_C)$$

$$V_{1R1} = V_{1R} \cdot ch(\gamma_{L2} \cdot L_{L2}) - I_{1R} \cdot Z_{C_{L2}} \cdot sh(\gamma_{L2} \cdot L_{L2}) \quad I_{1R1} = I_{1R} \cdot ch(\gamma_{L2} \cdot L_{L2}) - \frac{V_{1R}}{Z_{C_{L2}}} \cdot sh(\gamma_{L2} \cdot L_{L2})$$

### Fault in the cable

$$V_{1F} = V_{1L1} \cdot ch(\gamma_C \cdot d \cdot L_C) - I_{1L1} \cdot ZC_C \cdot sh(\gamma_C \cdot d \cdot L_C)$$

$$V_{1L1} = V_{1L} \cdot ch(\gamma_{L1} \cdot L_{L1}) - I_{1L} \cdot ZC_{L1} \cdot sh(\gamma_{L1} \cdot L_{L1}) \quad I_{1L1} = I_{1L} \cdot ch(\gamma_{L1} \cdot L_{L1}) - \frac{V_{1L}}{ZC_{L1}} \cdot sh(\gamma_{L1} \cdot L_{L1})$$

$$V_{1F} = V_{1R1} \cdot ch[\gamma_C \cdot (1-d) \cdot L_C] - I_{1R1} \cdot ZC_C \cdot sh[\gamma_C \cdot (1-d) \cdot L_C]$$

$$V_{1R1} = V_{1R} \cdot ch(\gamma_{L2} \cdot L_{L2}) - I_{1R} \cdot ZC_{L2} \cdot sh(\gamma_{L2} \cdot L_{L2}) \quad I_{1R1} = I_{1R} \cdot ch(\gamma_{L2} \cdot L_{L2}) - \frac{V_{1R}}{ZC_{L2}} \cdot sh(\gamma_{L2} \cdot L_{L2})$$

$\gamma_{L1}, \gamma_{L2}, \gamma_C$  - propagation constants for overhead sections 1 and 2 and cable respectively

$ZC_{L1}, ZC_{L2}, ZC_C$  - characteristic impedances for overhead sections 1 and 2 and cable respectively

$L_{L1}, L_{L2}, L_C$  - Lengths for the overhead sections 1 and 2 and cable respectively

The circuit considered by the fault locator algorithm for a fault located in the second overhead section is similar to the one considered for the first overhead section.

The algorithm must determine, first, the faulted section, to select the appropriate circuit. Reference [8] describes a fault locator for an overhead line divided in multiple sections. The faulted section is determined by calculating the distance to the fault from one of the line ends, and analyzing the value obtained. There are other fault locating algorithms to determine faults in three terminal lines [4], [5], and [6] or in distribution grids with intermediate loads [7], assuming a hypothetical fault location. For mixed lines it is possible to locate the faulted section in a similar fashion. The distance to the fault ( $d$ : from one of the cable ends – see figure 5) is calculated assuming that the fault is in the underground section. If the result is between 0 and 1, the assumption is confirmed and the block recloser signal is generated.

If the result is negative or greater than 1, the reclosing sequence is completed and the calculations are done considering the fault in the following overhead portion of the line:

- Overhead section 1 if  $d < 0$ : the voltage drop for the impedance  $d \cdot Z_{1C}$  included in the circuit of figure 5 would be negative, indicating that the current  $I_{1L1}$  should have opposite direction to the one in the figure.
- Overhead section 2 if  $d > 1$ : the voltage drop for the impedance  $(1-d) \cdot Z_{1C}$  included in the circuit of figure 5 would be negative, indicating that the current  $I_{1L2}$  should have opposite direction to the one in the figure.

Nevertheless, considering the possible errors of the fault locator described, the fault will be considered outside the cable when  $d > 1 \cdot K1$  and when  $d < K2$ . The constants  $K1$  and  $K2$  will be determined after simulations for each mixed line are performed.

Two algorithms will be considered, using the positive sequence fault magnitudes (algorithm 1) and those of pure fault values (algorithm 2), that is subtracting the pre-fault component. Pre-fault values will be recorded one or two cycles before the activation of the fault detector described in section 2.3.

### 3.1 Simulation

A 220kV mixed line is simulated using a RTDS. The line parameters are included in table 11. Different fault types are simulated with different fault resistance, and different incident angle. The positive sequence voltages and currents at both ends of the line are obtained using two PMUs, similar to the ones described in section 2.3.

Overhead Section 1 L=69.1 km	$z1 = 0.0717 + j \cdot 0.4135 \text{ } \Omega/\text{Km}$ $z0 = 0.3029 + j \cdot 1.2471 \text{ } \Omega/\text{Km}$ $y1 = j \cdot 2.8 \text{ } \mu\text{S}/\text{Km}$ $y0 = j \cdot 1.97 \text{ } \mu\text{S}/\text{Km}$
Cable L=3.9 km	$z1 = 0.0121 + j \cdot 0.1573 \text{ } \Omega/\text{Km}$ $z0 = 0.1089 + j \cdot 0.0484 \text{ } \Omega/\text{Km}$ $y1 = j \cdot 87.9 \text{ } \mu\text{S}/\text{Km}$ $y0 = j \cdot 87.9 \text{ } \mu\text{S}/\text{Km}$
Overhead Section 2 L=12.8 km	$z1 = 0.0718 + j \cdot 0.4144 \text{ } \Omega/\text{Km}$ $z0 = 0.3036 + j \cdot 1.2493 \text{ } \Omega/\text{Km}$ $y1 = j \cdot 2.8 \text{ } \mu\text{S}/\text{Km}$ $y0 = j \cdot 1.98 \text{ } \mu\text{S}/\text{Km}$

*Table 11. Simulated mixed line parameters*

#### 3.1.1 Results without external errors

Tables 12, 13 and 14 include some of the results obtained without taking into account external parameters to the PMUs, and considering faults without DC component. The maximum error recorded for faults in the first overhead section is 0.373%. Due to the smaller impedance per length unit of the cable (about 3 times less than the one for overhead sections) and the smaller length of the cable section itself, the fault locator has inferior accuracy for faults in the underground section. Results included in Table 12, for faults in the cable, have been obtained from values recorded 1 or 2 cycles after the activation of the fault detection unit (as explained in section 2.3). Calculations using values recorded at different times display errors up to 11%, therefore the algorithm is not suitable to locate faults in the cable. However, it should be noted that an 11% error relative to the cable impedance is equivalent to an error of 0.239% and 1.289% with respect to the impedance of the overhead sections 1 and 2 respectively. Additional cable faults have been simulated under different conditions, but the results have not been included in the paper due to the error dispersion recorded by reading values at different times after the fault detector is activated. In any case, all the errors relative to the impedance of the first overhead section are within the results shown in the tables for faults in such overhead section.

FAULTS IN OVERHEAD SECTION 1		
FAULT LOCATION	LOCATION ALGORITHM 1	LOCATION ALGORITHM 2
10%	10.037%	9.827%
20%	19.812%	19.990%
30%	29.923%	30.057%
40%	39.996%	40.172%
50%	49.803%	50.084%
60%	59.980%	60.139%
70%	70.191%	70.105%
80%	79.718%	79.861%
90%	90.042%	90.187%

FAULTS IN THE CABLE		
FAULT LOCATION	LOCATION ALGORITHM 1	LOCATION ALGORITHM 2
10%	14.256%	15.766%
20%	25.231%	26.320%
30%	32.489%	24.686%
40%	39.574%	37.963%
50%	51.527%	45.603%
60%	68.502%	66.456%
70%	77.820%	76.968%
80%	82.341%	83.563%
90%	93.042%	94.187%

*Table 12. Influence of fault location (fault type: AG, fault resistance: 10 ohms)*

FAULTS IN OVERHEAD SECTION 1			
FAULT TYPE	FAULT LOCATION	LOCATION ALGORITHM 1	LOCATION ALGORITHM 2
AG	20%	19.812%	19.990%
BG	20%	19.862%	20.168%
CG	20%	20.265%	20.373%
AB	20%	19.851%	20.013%
BC	20%	20.060%	20.110
CA	20%	20.275%	19.874%
ABG	20%	20.256%	19.855%
BCG	20%	19.823%	19.924%
CAG	20%	19.836%	19.960%
ABC	20%	20.005%	20.050%
AG	80%	79.718%	79.861%
BG	80%	79.981%	80.206%
CG	80%	80.219%	80.057%
AB	80%	80.186%	80.162%
BC	80%	80.237%	80.213%
CA	80%	80.257%	80.224%
ABG	80%	80.225%	80.201%
BCG	80%	79.633%	79.697%
CAG	80%	80.256%	80.233%
ABC	80%	80.040%	80.110%

*Table 13. Influence of the fault type (fault resistance: 10 ohms)*

FAULTS IN OVERHEAD SECTION 1				
FAULT TYPE	FAULT LOCATION	FAULT RESISTANCE (ohms)	LOCATION ALGORITHM 1	LOCATION ALGORITHM 2
AG	20%	10	19.812%	19.990%
BCG	20%	10	19.823%	19.924%
AG	20%	50	20.161%	20.187%
BCG	20%	50	20.173%	20.231%
AG	80%	10	79.718%	79.861%
BCG	80%	10	79.633%	79.697%
AG	80%	50	79.675%	80.041%
BCG	80%	50	79.814%	80.237%

**Table 14.** Influence of the fault resistance

### 3.1.2 Results with external errors

For faults located at different percentages of the first overhead section, the effect of some external factors to the PMUs are analyzed, such as uncertainties in the line parameters, potential synchronization errors between ends, and instrument transformer errors. DC component influence is also considered.

#### 3.1.2.1 Influence of the line parameters

Table 15 includes additional errors introduced by algorithms 1 and 2 when the positive sequence impedance is modified 10% in each section of the line. The worse case scenario has been considered, defined by:  $Z_{OH\_Section1} * 1.1 / Z_{cable} * 0.9 / Z_{OH\_Section2} * 0.9$ .

FAULT LOCATION	ADDITIONAL ERROR ALGORITHM 1	ADDITIONAL ERROR ALGORITHM 2
20%	-1.419%	-0.853%
40%	-2.256%	-1.716%
60%	-2.916%	-2.444%
80%	-3.485%	-3.060%

**Table 15.** Influence of a 10% error between line impedances

#### 3.1.2.2 Influence of synchronization between ends

Table 16.a includes the additional errors introduced by the algorithm 1 when there is a 10° phase difference between the currents measured by the PMUs. Table 16.b includes the additional errors when the 10° phase difference is between the voltages. In this last case, faults located at 20% of the section have an additional error of 16.245%, unacceptable for this application. This error is due to the high magnitude that the fault voltage has, as the faults injected were very resistive ones. That is why algorithm 2, based on pure fault values, barely introduces additional errors.

In any case, note that the use of GPS signals will reduce to a minimum the synchronization errors (in theory down to 1 us).

FAULT LOCATION	ADDITIONAL ERROR ALGORITHM 1	ADDITIONAL ERROR ALGORITHM 2	FAULT LOCATION	ADDITIONAL ERROR ALGORITHM 1	ADDITIONAL ERROR ALGORITHM 2
20%	0.024%	-0.182%	20%	16.245%	0.021%
40%	0.517%	-0.169%	40%	15.283%	0.003%
60%	1.173%	-0.06%	60%	14.461%	0.025%
80%	1.615%	0.02%	80%	14.425%	0.007%

**16.a)** Synchronization error between currents **16.b)** Synchronization error between voltages

**Table 16.** Influence of a 10° synchronization error between ends

### 3.1.2.3 Influence of the current transformers

Table 17 includes the additional errors introduced by algorithm 1 when errors of 3% and 2° are added to the magnitude and angle of the currents measured by the PMUs. The worse case scenario is considered, being those where both local and remote currents have the maximum error with opposite sign (+3% for  $I_{local}$  / -3% for  $I_{remote}$ ) and errors in the angle with the same sign (+2° for  $I_{local}$  / +2° for  $I_{remote}$ ).

FAULT LOCATION	ADDITIONAL ERROR ALGORITHM 1
20%	-0.791%
40%	-1.425%
60%	-1.75%
80%	-1.742%

**17.a)** 3% magnitude error

FAULT LOCATION	ADDITIONAL ERROR ALGORITHM 1
20%	0.230%
40%	0.377%
60%	0.442%
80%	0.426%

**17.b)** 2° angle error

**Table 17.** Influence of the current transformers

### 3.1.2.4 Influence of the voltage transformers

Table 18 includes the additional errors introduced by algorithm 1 when errors of 3% and 2° are added to the magnitude and angle of the voltages measured by the PMUs. The worse case scenario is considered, being those where both local and remote voltages have the maximum error with opposite sign in the magnitudes (+3% for  $V_{local}$  / -3% for  $V_{remote}$ ) or angle (+2° for  $V_{local}$  / -2° for  $V_{remote}$ ).

FAULT LOCATION	ADDITIONAL ERROR ALGORITHM 1
20%	6.343%
40%	9.457%
60%	10.757%
80%	10.198%

**18.a)** 3% magnitude error

FAULT LOCATION	ADDITIONAL ERROR ALGORITHM 1
20%	7.393%
40%	7.452%
60%	7.363%
80%	7.226%

**18.b)** 2° angle error

**Table 18.** Influence of the voltage transformers

Considering the previous results, it is required to compensate for the errors introduced by the voltage transformers. The best approach is to calibrate the PMUs according to the error curves of the voltage transformer used. However it should be noted that, for the faults injected, algorithm 2 will considerably reduce such errors.

#### 3.1.2.5 *Influence of the incidence angle*

Considering the worse case scenario, with current readings 1 cycle after the activation of the fault detector and maximum offset, the error introduced in the current is 1% in the magnitude and 3° in the angle. This error gives an additional maximum error in the fault locator of 0.383% for faults at 80% of the overhead section 1.

These results, and taking into account that the PMUs will be calibrated according to the instrument transformer error curves (mainly the voltage transformers), imply an important improvement with respect to the solution based on distance zones.

## 4 DYNAMIC BEHAVIOR MONITORING

The continuous growth and the increase of interconnections between electric systems have a direct impact on the system stability. The "Union for the Co-ordination of Transmission of Electricity" (UCTE) is the association of transmission system operators in continental Europe. There are small signal oscillations in the UCTE system, in the range of 0.2 Hz, which create problems such as:

- ✓ Unplanned energy flows in the UCTE grid
- ✓ Uncertainty on the dynamic behavior of the system due to improper damping of such oscillations

On another front, the rapid growth of wind generation in the Iberian Peninsula, introduces further uncertainties to the dynamic behavior of the system. An important number of conventional generators equipped with PSS (Power System Stabilizers) are being replaced by wind generators, with potential changes to the dynamic behavior of the system.

This new environment creates the need for improving the knowledge of such dynamic behavior. This can be achieved by direct observation as well as additional system analysis via system modeling.

A pilot project is underway, using phasor measurement units (PMUs) in an application to determine the following modal characteristics of the interconnection Spain-Morocco:

- ✓ Modal frequency
- ✓ Amplitude of different modes
- ✓ Damping
- ✓ Phase

Figure 6 depicts the main functional components of the system.

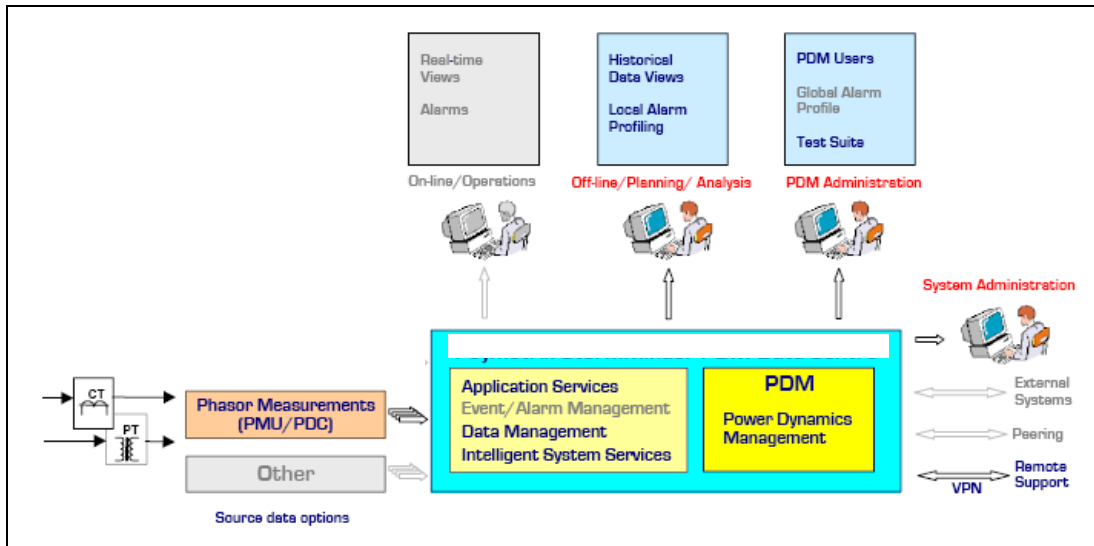


**Figure 6.** Grid Dynamic Behavior Monitoring System

Two PMUs are installed in the double circuit 400 kV cable that interconnects Spain and Morocco to continuously monitor the current and voltage. The sampling rate is 50 phasors per second.

These devices are synchronized via a GPS clock with direct connection to the PMU. The GPS clock has at least an accuracy of 100 us. The metering from the PMUs is sent in real time via the REE communications network to a server where the application in charge of processing the phasor data is located. Figure 7 depicts the communication architecture developed for this project.

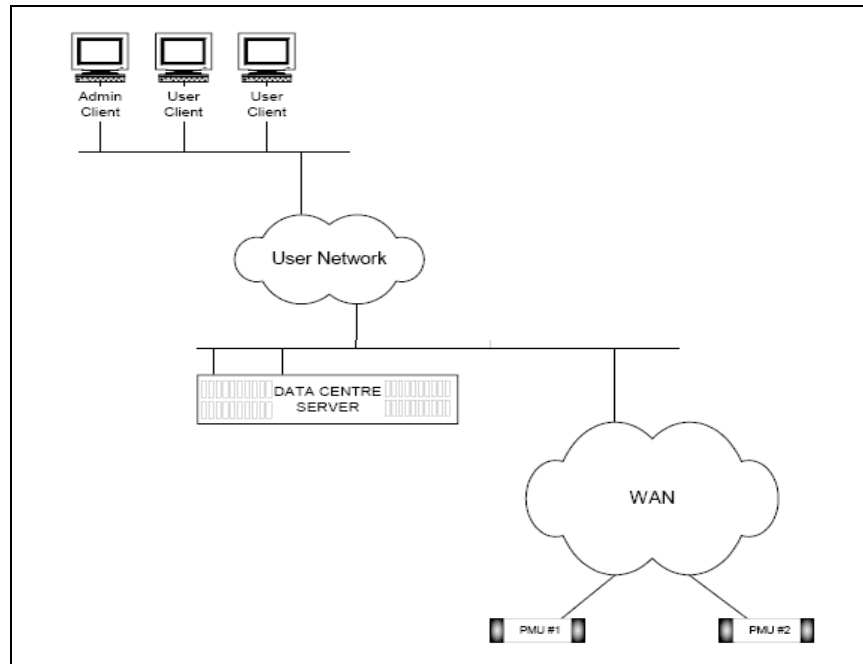


**Figure 7.** PMU Communication System Architecture

Based on this system and with the data provided by the PMUs, REE will be able to:

- ✓ Study potential damping problems in the system, identifying local and inter-area oscillation modes. This requires continuous monitoring of the amplitude of the oscillation modes and its damping.
- ✓ Retuning of the PSS in the power plants. Observing the damping of the different oscillation modes will be useful to revise the PSS settings in power stations.
- ✓ Model validation. Continuous monitoring of the system dynamics will provide the necessary data to validate models of the different operating conditions of the system.
- ✓ Improvement of system security. Analyzing the phasor data will be possible to establish corrective action plans against unstable oscillations.

## CONCLUSION

This paper describes the synchrophasor measurement device applications devised by Red Eléctrica de España in the short term.

Line impedances calculation based on PMUs can provide better results than traditional methods, based on the line constants. PMUs require high accuracy in the synchronization and need to be calibrated with instrument transformers errors. Positive sequence impedance calculation based on fault / pure fault values allows higher synchronization errors between the voltages and higher VT errors.

Fault locator for mixed lines based on PMUs can be used as a protection scheme without devices required at both ends of the cable. For the faults injected, the algorithm based on pure fault values allowed higher synchronization errors between the voltages and higher VT errors.

Oscillations monitoring based on PMUs improves knowledge of system dynamic behaviour.

## BIBLIOGRAPHY

- [1] Líneas de Transporte de Energía – L. M. Checa, Marcombo S.A. 01/01/1988
- [2] Analysis of Faulted Power Systems – Paul M. Anderson IEEE Press Power Systems Engineering Series
- [3] Handbook of Power System Engineering – Yoshihide Hase, WILEY 2007
- [4] “A New Fault Location Technique for Two- and Three-Terminal Lines”- Girgis, A.A.; Hart, D.G.; Peterson, W.L.- IEEE Transactions on Power Delivery, Volume 7, Issue 1, Jan 1992 Page(s):98 – 107
- [5] “A Practical Approach to Accurate Fault Location on Extra High voltage Teed Feeders” - Aggarwal, R.K.; Coury, D.V.; Johns, A.T.; Kalam, A.- IEEE Transactions on Power Delivery, Volume 8, Issue 3, Jul 1993 Page(s):874 – 883
- [6] “Development of a new fault location system for multi-terminal single transmission lines” - Abe, M.; Otsuzuki, N.; Emura, T.; Takeuchi, M. - IEEE Transactions on Power Delivery, Volume 10, Issue 1, Jan 1995 Page(s):159 – 168
- [7] “Fault location method for MV cable network” - Saha, M.M.; Provoost, F.; Rosolowski, E. Developments in Power System Protection, 2001, Seventh International Conference on (IEE) Volume , Issue , 2001 Page(s):323 – 326
- [8] “Development of an advanced transmission line fault location system.II. Algorithm development and simulation” - Lawrence, D.J.; Cabeza, L.Z.; Hochberg, L.T. - IEEE Transactions on Power Delivery, Volume 7, Issue 4, Oct 1992 Page(s):1972 – 1983
- [9] “Evaluation and development of transmission line fault-locating techniques which use sinusoidal steady-state information,” - E.O. Schweitzer III *Ninth Annual Western Protective Relay Conference*, Spokane, Washington, Oct. 1982.
- [10] “Challenges and Solutions in the Protection of a Long Line in the Furnas System” – R. Abboud, W. Ferreira, F.Goldman - Western Protective Relay Conference, Spokane, WA, October, 2005
- [11] “Protective Relaying Considerations for Transmission Lines With High Voltage AC Cables” - Working Group D12 of the Line Protection Subcommittee, PSRC - IEEE Trans. Power Delivery, vol. 12, No. 1, pp. 83– 96, Jan. 1997
- [12] “Adapting Protection to Frequency Changes” – R. Cimadevilla, R. Quintanilla, S. Ward - Western Protective Relay Conference, Spokane, WA, October, 2005
- [13] EMTP Theory Book – H. W. Dommel – BPA 1987

## **AUTHOR BIOGRAPHYS**

**Mr. Jorge Gómez-Salas** graduated in Telecommunication Engineering from the Superior Engineering College of Madrid, Spain in 1999. He obtained a degree in “Telecommunication Companies Management” in 2002. Mr. Gomez obtained a master’s degree in “Electrical Energy Generation Technologies” in 2003. He also obtained a degree in “Economy of the Energy Sector” in 2007. Mr Gomez has been working for the Red Electrica de España (REE - National Electric System Operator of Spain) as a Protection Relay Engineer since 2003. He is mainly focused in setting and coordinating transmission transformer and line protective relays.

**Mr. Santiago López-Barba** graduated in Mining Engineering majoring in Energy and Fuels and MPhil in Power System Engineering by UMIST (University of Manchester Institute of Science and Technology). Mr. Lopez-Barba is responsible for protection and network security analysis and incident reporting in Red Electrica de España (REE - National Electric System Operator of Spain), with expertise in power systems Security Issues and Power Systems Operations. From 1998 to 2002 he worked in Arthur Andersen Consulting as manager of projects in the utility sector (regulations, operation markets design, and economic-consulting), and previously he worked as a control system engineer for power plants. Currently, Santiago is developing projects in the field of PMU technology, focusing in the wide area protection systems and oscillatory instability detection as an area under his actual responsibilities in REE.

Mr Lopez-Barba is a member of the IEEE Power Engineering Society and the IEEE Communications Society. With large experience in the power systems operations, he has participated in the ancillary services market design of the Spanish TSO (Imbalance market). He has been the manager in charge of the Privatization Design and Stranded Cost Calculations of Power Generating Company of Slovakia from 2001 to 2002 and in the SET (Slovakia TSO) business units organization. He was engaged in the process of market recovery mechanism implementation of the sunk cost of the Polish Electricity System and Operational Procedures for the market liberalization process.

**Mr. Roberto Cimadevilla** graduated in Electrical Engineering from the Superior Engineering College of Gijón, Spain in 2001. He later obtained a master’s degree in “Analysis, simulation and management of electrical power systems” from the University of País Vasco, Spain. He previously worked for the Red Electrica de España (REE - National Electric System Operator of Spain) as a Protection Relay Engineer. Roberto is with ZIV since the beginning of 2003 as an Application Engineer, being responsible in this area for the development of a new distance relay and a Phasor Measurement Unit. He has written several technical papers, some of them presented at international conferences.

**Mr. Oscar Bolado** is the manager of ZIV USA Inc. in charge of the marketing, sales, customer service, and engineering and technical support activities of the company. With previous experience in power system maintenance, Oscar joined ZIV in 1999 as an application and sales engineer. He is a senior member of IEEE, and member of the Power Systems Relaying Committee. Oscar graduated in Electrical Engineering from Western Michigan University and is a 2008 MBA candidate at DePaul University.